Applied Physics Letters

Quasi-coherent thermal radiation with multiple resonant plasmonic cavities

Cite as: Appl. Phys. Lett. **109**, 261101 (2016); https://doi.org/10.1063/1.4972965
Submitted: 11 October 2016 . Accepted: 11 December 2016 . Published Online: 27 December 2016

Chun Yen Liao, Chih-Ming Wang, Bo Han Cheng, Yi-Hao Chen, Wei-Yi Tsai, De-Yu Feng, Ting-Tso Yeh, Ta-Jen Yen, and Din Ping Tsai

Quasi-coherent thermal radiation with multiple resonant plasmonic cavities

Chun Yen Liao,[1] Chih-Ming Wang,[2,a)] Bo Han Cheng,[3] Yi-Hao Chen,[1] Wei-Yi Tsai,[1] De-Yu Feng,[2] Ting-Tso Yeh,[4] Ta-Jen Yen,[4] and Din Ping Tsai[1,5,a)]
[1]*Department of Physics, National Taiwan University, Taipei 106, Taiwan*
[2]*Department of Opto-Electronic Engineering, National Dong Hwa University, Hualien 974, Taiwan*
[3]*Department of Electro-Optical Engineering, National Taipei University of Technology, Taipei 106, Taiwan*
[4]*Department of Materials Science and Engineering, National Tsing Hua University, Hsinchu 300, Taiwan*
[5]*Research Center for Applied Sciences, Academia Sinica, Taipei 115, Taiwan*

(Received 11 October 2016; accepted 11 December 2016; published online 27 December 2016)

This paper proposes a 1D plasmonic multilayer structure as a high-contrast mid-infrared thermal emitter with three distinct resonant wavelengths. The three resonance modes, based on the localized surface plasmon, provide an omnidirectional thermal emission. The emissivity spectrum reveals high polarization and strongly angle-independent properties. The resonance-assisted emissivity can be as high as 19.5 dB relative to off-resonant sideband emissivity. Such extremely low sideband emissivity makes the proposed plasmonic thermal emitter an efficient, high-contrast emitter, which will be useful for thermophotovoltaic and thermal sensing applications. *Published by AIP Publishing.*
[http://dx.doi.org/10.1063/1.4972965]

Coherent mid-infrared (MIR) light sources with designable and spectra are in high demand for thermal sensing and energy harvesting applications.[1–3] Multi-band wide-angle absorption/thermal emission is required for many applications, such as IR sensors and integrated multi-functional devices. In the MIR spectral range, the usefulness of quantum cascade lasers or light-emitting diodes (LED) as radiating sources is limited by their low efficiency and high cost.[4–7] Conventional methods for obtaining coherent MIR light sources including using introduced filters to pick up narrow-band wavelengths that are thermally emitted by heated material, as in the incandescent light bulbs. Nevertheless, only a small fraction of the energy is extracted from the wide spectral range of light bulbs, so most of the radiation is wasted. Since various approaches, such as those that involve microcavity resonance, nano antennas, multilayer systems, photonic crystals, surface plasmon polaritons (SPPs) and the excitation of surface phonon polaritons, have been utilized to manipulate the spectral distribution and polarization of thermal radiation, coherent thermal emission light sources that are based on the designed nanostructures have attracted substantial interest.[8–19] Plasmonic thermal emitters (PTEs) that are based on a few layers of a periodic metallic structure provide much narrower radiation peaks than black-body emitters at the same temperature.[20,21] PTEs have advantages over currently available MIR light sources, including their low cost, high power, simplicity of fabrication, high efficiency, and relatively low sideband emission.[22,23] Furthermore, a PTE can be simply heated by directly applying a DC or AC current, and the electric power is directly converted into radiation. Metamaterials, which are electromagnetic media on a sub-wavelength scale, provide additional opportunities for manipulating light across the entire electromagnetic spectrum.

After the development of incandescent light bulb by Thomas Alva Edison, lighting became essential to human society. The development of LEDs has almost signaled the demise of conventional incandescent light bulbs. However, if its unwanted spectrum can be suppressed, an incandescent light bulb can still be a cost-effective light source. Here, a one-dimensional (1D) structure is utilized to support triple resonances. Such a 1D structure is easier to fabricate than a two-dimensional structure with triple resonances, and it exhibits a higher polarization selectivity. In this work, a plasmonic absorber with three designable resonance modes and a 1D metallic structure is designed and fabricated. The thermal radiation properties of a device are directly related to its absorption features in thermodynamic equilibrium. According to the Kirchhoff's law of thermal radiation, the angular and frequency-dependent emittance of an object is equal to its frequency-dependent absorptance. The use of a designed absorber as a functional emitter is therefore straightforward. The proposed PTE exhibits omnidirectional resonance properties with a high quality factor (Q-factor). Its simulation agrees reasonably with experimental results.[24–26] We believe that choosing a suitable material and further reducing the resonance wavelength to the visible regime, can cause the structure to act as a high-efficiency light source with the three primary colors.

Figure 1(a) schematically depicts the triple-wavelength thermal emitter. The structure consists of a 1D grating and a 1D T-shaped grating. The metallic structure is made of gold (Au). The dielectric material is spin-on glass (SOG), which is assumed to be SiO_2. A substrate is coated with an optically thick Au film to serve as a semi-infinite mirror. A thin dielectric insulator layer with a thickness of T_{SOG} forms a gap between the upper metallic structures and the bottom Au film. The plasmonic multilayer structure can be treated as a cascade of metal/insulator/metal (MIM) cavities in the x-direction. The periodicity of the structure is denoted as Λ_g. The widths at the top and the bottom of the T-shaped metallic line are W_T and T_W, respectively. The width of the metallic grating is denoted as W_g.

The proposed PTE with triple resonances was fabricated on a silicon substrate. First, a 100 nm-thick Au film was

a)Authors to whom correspondence should be addressed. Electronic addresses: wangcm@mail.ndhu.edu.tw and dptsai@phys.ntu.edu.tw

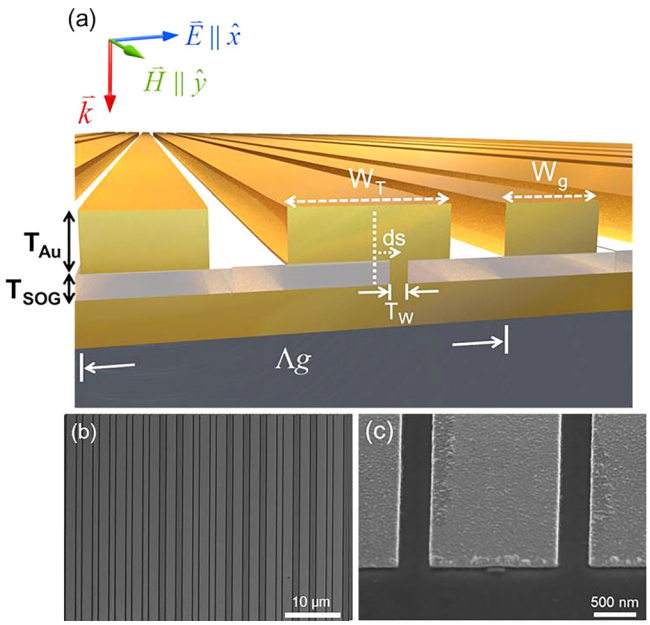

FIG. 1. Plasmonic thermal emitter. (a) Schematic representation of PTE. Thickness of SOG layer is denoted as T_{SOG}. Width of Au grating is denoted as W_g. Widths of top and bottom of the T-shaped metallic line are W_T and T_W, respectively. Period of Au 1D nanostructure is denoted as Λ_g. Geometric parameters of the structure are $\Lambda_g = 3\,\mu$m, $W_g = 0.5\,\mu$m, $W_T = 2\,\mu$m, $T_w = 0.2\,\mu$m, $ds = 0.23\,\mu$m, and $t_{Au} = 0.1\,\mu$m. (b) SEM image of top view of PTE. (c) SEM image of side view of PTE.

deposited on the substrate by sputtering. Then, a grating, functioning as the pillar in a T-shaped structure, was formed on the Au film using electron beam (EB) lithography and the lift-off technique. To generate a robust dielectric spacer within the two metallic layers, a dielectric layer was coated onto the pillar structure using spin-on glass (SOG). The SOG can fully cover the pillar structure and form a flat dielectric surface by spin coating method. Finally, the top metallic structure was made on the dielectric surface using EB lithography and the lift-off technique. The size of the triple resonance emitter was $150\,\mu\text{m} \times 150\,\mu\text{m}$, which was sufficiently large to obtain clear signals from the structure using a Fourier-transform infrared microscope (μ-FTIR). Figures 1(b) and 1(c) display scanning electron microscopy (SEM) images of the triple resonance emitter. The lengths of the MIM cavities are indicated. The lengths of the three MIM cavities are $W_g = 500\,\text{nm}$, $(W_T - T_W)/2 - ds = 670\,\text{nm}$, and $(W_T - T_W)/2 + ds = 1130\,\text{nm}$.

The optical properties of the structure are calculated using commercial software that is based on finite-difference time domain (FDTD). The input light is x- (or y-) polarized, so its electric field is normal (parallel) to the grating grooves. The incident light impinges on the structure from the top. The dispersive complex dielectric constants of Au are taken from Ref. 26. The dielectric constant of the SOG is assumed to be non-dispersive with a fixed value of $\varepsilon = 1.9309$, which is very close to the dielectric constant of SiO_2 at $4\,\mu$m.

The emissivity (absorptivity), of the PTE is first characterized. The emissivity is measured with a μ-FTIR with a reflective microscope objective with a magnification of 36×. A liquid N_2-cooled HgCdTe infrared detector is used to detect radiation. Since the background of the PTE is an optically thick Au film, its transmission is zero. Therefore, the emissivity $\alpha(\omega)$ can be simply obtained as $\alpha(\omega) = 1 - R(\omega)$ for a sub-wavelength structure. Figure 2 presents the emissivity spectrum of the proposed structure for normally incident light. Black and red solid lines represent the spectra under x-polarized and y-polarized illumination, respectively. Solid and dotted lines represent the experimental and simulated results, respectively. As expected, no resonance mode exists for y-polarization light, according to both experimental and simulated results. As shown in Fig. 2(a), under x-polarized illumination, the structure supports the three resonance peaks at $\lambda = 2.14\,\mu$m, $\lambda = 3.3\,\mu$m, and $\lambda = 5.95\,\mu$m, which are denoted, for convenience, as D_1, D_2, and D_3, respectively. The peak values of the three resonance peaks are 51%, 79%, and 78%, respectively. The Q-factors of the D_1, D_2, and D_3 peaks are 10.25, 7.13, and 8.13, respectively. The emissivity (reflectance) in the MIR range must be suppressed for a high-contrast thermal emitter. Notably, y-polarization is associated with low emissivity and x-polarization is associated with the off-resonance condition. The mean emissivity for y-polarization within a spectral range from $5\,\mu$m to $10\,\mu$m can be as low as $0.88\% + 0.28$, owing to Au in MIR. As a result, the difference between the resonance emissivity and the sideband emissivity can be as high as 19.5 dB. The extremely low sideband emissivity makes the proposed PTE an efficient and high-contrast emitter.

Figure 2(b) presents the simulated emissivity spectrum. The simulation spectrum is similar to the measured one. Three resonance modes at $\lambda = 1.9\,\mu$m, $\lambda = 3.5\,\mu$m, and $\lambda = 5.9\,\mu$m are observed. However, since the precise dielectric constant of SOG in the MIR is unknown, it is assumed to be $\varepsilon = 1.9309$ without loss and dispersion. Consequently, the inherent absorption at $1.2\,\mu$m due to the absorption of SiO_2 phonon vibrations cannot be predicted in the simulation. Additionally, the resonance properties, such as peak position, contrast, and Q-factors, cannot be fitted well. Notably, the delocalized SP at $\lambda = 3\,\mu$m, shown in Fig. 2(b), is difficult to observe under focused illumination because the delocalized SP is highly dispersive in both angle and wavelength. The optical response of the sharp delocalized SP peak is averaged under focused light.

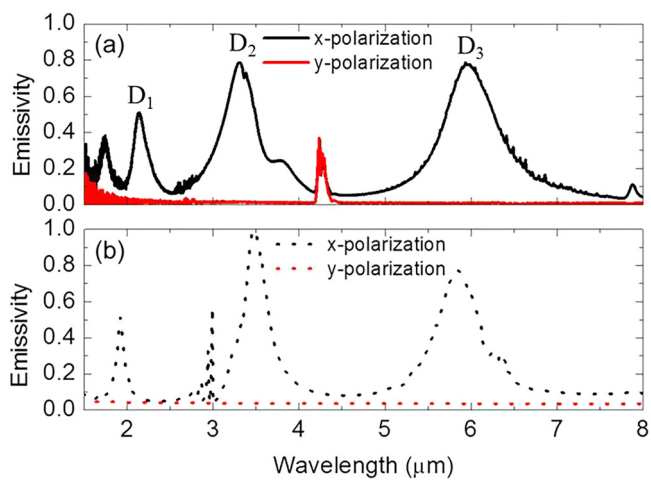

FIG. 2. Emissivity spectrum of proposed PTE. (a) Experimental results. (b) Simulated results. Black and red spectra were obtained under x-polarized and y-polarized illumination, respectively.

To elucidate more clearly, the nature of the triple resonant modes of our designed structure, the distributions of the magnetic field components at the three resonances were simulated. Figures 3(a)–3(c) plot the H_y field distribution at the resonance dips of D_1, D_2, and D_3 (as shown in Fig. 2), respectively. The H_y field of D_1 is localized within the two open-end MIM cavities that are formed by the metallic grating. The H_y field of D_2 and D_3 is localized within the MIM cavity, with one open end and one opposite-closed end that is formed by the T-shaped grating. Such resonance modes are also called gap-plasmon-guided mode. The resonance properties of the plasmon-guided modes depend strongly on the separation of the two adjacent metallic structures. Gap-plasmon-guided modes can be generated at small separations and highly localized in the tiny gap between two metallic structures. As mentioned above, the lengths of the three individual cavities that support D_1, D_2, and D_3 modes are $W_g = 500\,\text{nm}$, $(W_T - T_W)/2 - ds = 670\,\text{nm}$, and $(W_T - T_W)/2 + ds = 1130\,\text{nm}$, respectively. Due to the intrinsic optical property of plasmon based structures, the resonance wavelength can be purposely selected by tuning the feature dimensions of MIM cavity (see supplementary material).

The three cavities with different lengths support resonance modes with different wavelengths, and each cavity contains a strongly confined field. The localized fields in the neighboring cavities are not coupled, despite the small separation between the cavities. The resonances primarily yield excitation of magnetic dipole resonance owing to the circulating currents in the top and bottom metallic structures. Evidently, the electromagnetic energy of incident light can be confined efficiently within the cavities of the asymmetric structure at the corresponding resonance wavelength and dissipated by ohmic heating of the metallic parts. Therefore, the resonance-enhanced ohmic heating loss can result in a quasi-coherent emission peak.

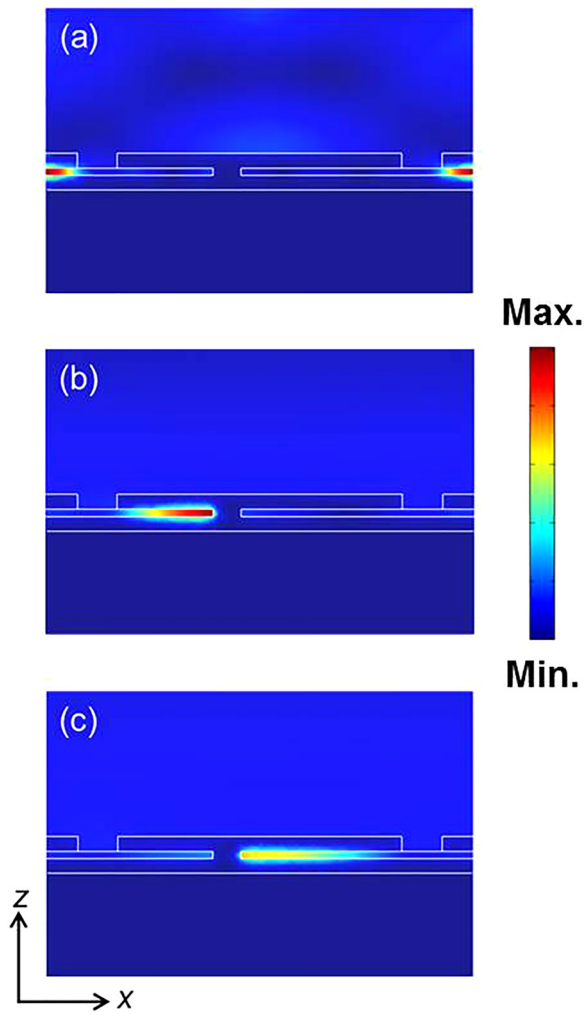

FIG. 3. H_y field distribution at various resonance wavelengths. (a)–(c) Simulated field at wavelengths of $\lambda = 2.1\,\mu\text{m}$, $\lambda = 3.2\,\mu\text{m}$, and $\lambda = 5.9\,\mu\text{m}$, respectively.

To identify the angle-dependent properties of the PTE, two objective lenses with a magnification of 15× and 36× are simply used to measure the spectral response. The half collection angles of the 15× and 36× lenses are 16° and 24°, respectively. Accordingly, the 36× lens can collect and average a larger solid angle than the 15× one. In Fig. 4(a), the black and red solid lines indicate the emissivity that is measured using the 15× and 36× objectives, respectively. The peak wavelengths and Q-values of the resonance at $\lambda = 3.3\,\mu\text{m}$ for the two lenses are almost equal. In the mode at $\lambda = 5.95\,\mu\text{m}$, the peak wavelength is the same while the Q-value is slightly reduced. In the mode at $\lambda = 2.16\,\mu\text{m}$, the peak wavelength is slightly redshifted to $\lambda = 2.21\,\mu\text{m}$, revealing that the resonance mode at $\lambda = 2.14\,\mu\text{m}$ is less localized than that of the other two modes. Figure 4(b) shows the simulated emissivity as a function of the incident angle. The D_3 mode remains almost constant as the incident angle varies. The delocalized SP peak is close to the resonance wavelength of the D_2 mode. When off-normally incident light impinges the structure, the delocalized SP peak splits and shifts. The delocalized SP is coupled to the D_2 mode, the delocalized and localized mode hybridization suppresses the emissivity, as shown in the range $\theta = -10°$ and $\theta = 10°$, because the delocalized SP couples out the localized mode within the MIM cavity at a specific incident angle. As a result, the resonance absorption is suppressed. However, since the measured spectrum is angle-averaged, the hybridization of delocalized and localized modes can barely be observed. Additionally, the simulation demonstrates that the wavelength is shifted by 1.5% as the incident angle increases from 0° to 30°, agreeing fairly well with the measurements.

In summary, this work demonstrated a high-contrast PTE that is based on a 1D plasmonic multilayer structure

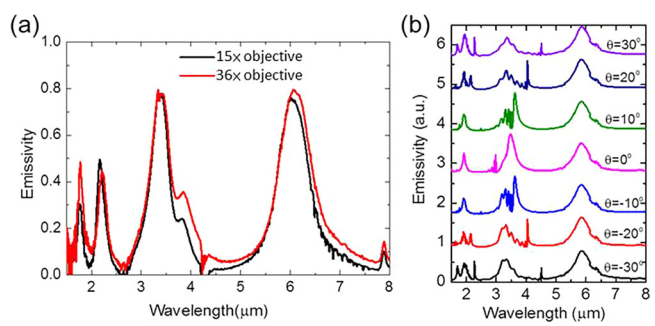

FIG. 4. Emissivity spectra of PTE. (a) Experimentally measured using objective lens with a magnification of 15× (36×). (b) Simulated emissivity spectra. From bottom to top, incident angle increases from −30° to 30° in increments of 10°.

that can thermally emit radiation of three wavelengths in the MIR region. The difference between its resonance emissivity and off-resonant sideband emissivity can be as high as 19.5 dB. The extremely low sideband emissivity makes the proposed PTE an efficient and high-contrast emitter, which will be useful for thermophotovoltaic and thermal sensing applications. The three resonance modes that are based on the localized surface plasmon provide omnidirectional thermal emission. The periodic patterned structures can be manipulated to realize a triple-band, wide-angle, polarization-dependent, quasi-coherent light source at three resonance wavelengths. The resonance modes are not coupled and so can be designed individually, facilitating the shortening of resonance wavelengths.

See supplementary material for the fabrication process, numerical simulation, emissivity measurement, the correlation between the resonant frequencies, and the geometry of proposed plasmonic thermal emitter, and the numerical emissivity spectra at different incident angles.

The authors acknowledge financial support from the Ministry of Science and Technology, Taiwan (Grant Nos. 105-2745-M-002-005-ASP, 105-2112-M-027-002-MY3, 104-2221-E-259-028-MY3, and 102-2120-M-259-002) and Academia Sinica (Grant No. AS-103-TP-A06). They are also grateful to the National Center for Theoretical Sciences, Molecular Imaging Center of National Taiwan University, National Center for High-Performance Computing, Taiwan, and Research Center for Applied Sciences, Academia Sinica, Taiwan for their supports.

[1]D. N. Kendall, *Applied Infrared Spectroscopy* (New York, Reinhold, 1966).
[2]A. D. Lenert, M. Bierman, Y. Nam, W. R. Chan, I. Celanović, M. Soljačić, and E. N. Wang, Nat. Nanotechnol. **9**, 126–130 (2014).
[3]M. D. Zoysa, T. Asano, K. Mochizuki, A. Oskooi, T. Inoue, and S. Noda, Nat. Photonics **6**, 535–539 (2012).
[4]V. V. Sherstnev, A. M. Monakhov, A. Krier, and G. Hill, Appl. Phys. Lett. **77**, 3908–3910 (2000).
[5]B. A. Matveev, N. V. Zotova, N. D. Il'inskaya, S. A. Karandashev, M. A. Remennyi, N. M. Stus', and G. N. Talalakin, J. Mod. Opt. **49**, 743–756 (2002).
[6]J. S. Yu, S. R. Darvish, A. Evans, J. Nguyen, S. Slivken, and M. Razeghi, Appl. Phys. Lett. **88**, 041111 (2006).
[7]C. L. Canedy, W. W. Bewley, J. R. Lindle, C. S. Kim, M. Kim, I. Vurgaftman, and J. R. Meyer, Appl. Phys. Lett. **88**, 161103 (2006).
[8]S. Maruyama, T. Kashiwa, H. Yugami, and M. Esashi, Appl. Phys. Lett. **79**, 1393–1395 (2001).
[9]K. Ikeda, H. T. Miyazaki, T. Kasaya, K. Yamamoto, Y. Inoue, K. Fujimura, T. Kanakugi, M. Okada, K. Hatada, and S. Kitagawa, Appl. Phys. Lett. **92**, 021117 (2008).
[10]J. A. Schuller, T. Taubner, and M. L. Brongersma, Nat. Photonics **3**, 658–661 (2009).
[11]C.-M. Wang and D.-Y. Feng, Opt. Express **22**, 1313–1318 (2014).
[12]C.-M. Wang and D. P. Tsai, IEEE J. Sel. Top. Quantum Electron. **19**, 4601005 (2013).
[13]K. A. Arpin, M. D. Losego, A. N. Cloud, H. Ning, J. Mallek, N. P. Sergeant, L. Zhu, Z. Yu, B. Kalanyan, G. N. Parsons, G. S. Girolami, J. R. Abelson, S. Fan, and P. V. Braun, Nat. Commun. **4**, 2630 (2013).
[14]S.-Y. Lin, J. G. Fleming, E. Chow, J. Bur, K. K. Choi, and A. Goldberg, Phys. Rev. B **62**, R2243–R2246 (2002).
[15]J. J. Greffet, R. Carminati, K. Joulain, J. P. Mulet, S. Mainguy, and Y. Chen, Nature **416**, 61–64 (2002).
[16]C.-M. Wang, Y.-C. Chang, M.-W. Tsai, Y.-H. Ye, C.-Y. Chen, Y.-W. Jiang, S.-C. Lee, and D. P. Tsai, IEEE Photonics Technol. Lett. **20**, 1103–1105 (2008).
[17]B. J. O'Regan, Y. Wang, and T. F. Krauss, Sci. Rep. **5**, 13415 (2015).
[18]C.-W. Cheng, M. N. Abbas, Z.-C. Chang, M. H. Shih, C.-M. Wang, M. C. Wu, and Y.-C. Chang, Opt. Lett. **36**, 1440 (2011).
[19]T. Inoue, M. D. Zoysa, T. Asano, and S. Noda, Appl. Phys. Lett. **108**, 091101 (2016).
[20]C.-M. Wang, Y.-C. Chang, M.-N. Abbas, M.-H. Shih, and D. P. Tsai, Opt. Express **17**, 13526–13531 (2009).
[21]C.-M. Wang, Y.-C. Chang, M.-W. Tsai, Y.-H. Ye, C.-Y. Chen, Y.-W. Jiang, Y.-T. Chang, S.-C. Lee, and D. P. Tsai, Opt. Express **15**, 14673–14678 (2007).
[22]G. Biener, N. Dahan, A. Niv, V. Kleiner, and E. Hasmana, Appl. Phys. Lett. **92**, 081913 (2008).
[23]X. Shen, Y. Yang, Y. Zang, J. Gu, J. Han, W. Zhang, and T. J. Cui, Appl. Phys. Lett. **101**, 154102 (2012).
[24]X. Shen, T. J. Cui, J. Zhao, H. F. Ma, W. X. Jiang, and H. Li, Opt. Express **19**, 9401–9407 (2011).
[25]R. Siegel and J. Howell, *Thermal Radiation Heat Transfer* (Hemisphere, 1981).
[26]E. D. Palik, *Handbook of Optical Constants of Solids* (Academic Press, New York, 1985).